APF-based Real-Time Cooperative Collision Avoidance for n-DOF Manipulators

Erick J. Rodríguez-Seda and Michael M. D. Kutzer
United States Naval Academy, MD, USA
{rodrigue,kutzer}@usna.edu

***Abstract*—This paper presents a decentralized, cooperative, real-time avoidance control strategy for rigid manipulators. The proposed avoidance control law builds on the concepts of artificial potential field functions and provides tighter bounds on the minimum safe distance compared to traditional potential-based controllers. Moreover, the control law is given in analytical, continuous closed-form, avoiding the use of optimization techniques and discrete algorithms. It is rigorously proven to guarantee collision avoidance at all times. A simulation example of two manipulators with cylindrical links under the proposed avoidance control law is given.**

I. Introduction

Robotic manipulators are used in a wide range of applications, such as sorting facilities, construction, and health care, to name a few [1]. In all these scenarios, the manipulators must interact with their environment that may include obstacles, people, and other robots. For example, consider the two articulated robots in Fig. 1. The robots need to avoid collisions not only with static and dynamic objects in their environment but also with other robots and with themselves. Therefore, it is critical to develop control protocols that can guarantee the safety of the manipulators at all times.

Of particular interest are distributed real-time collision avoidance controllers that are provably safe. For instance, frameworks based on artificial potential fields (APF) [3] can be implemented in a decentralized manner and can be rigorously proven to avoid collision by applying Lyapunov theory. Recent examples include [5, 8]. A common drawback of these approaches is the modeling of links and segments of obstacles as spheres, a collection of spheres [6, 7], or other primitive shapes [9], which may lead to the implementation of several APF functions or unnecessary conservatism due to the convex approximations. Other approaches introduce the idea of critical points along the surfaces of obstacles[8], which in turn can result in control discontinuities.

In this paper, we propose an APF method for rigid manipulators. The control law is decentralized, since only information from other robots and obstacles within a bounded distance is considered, and cooperative, given that it guarantees collision avoidance if other robots and dynamics agents abide by the same control policy [4]. The novelty of the approach is the proposal of a shape- and orientation-dependent continuously differentiable minimum safe distance between two links or obstacles that yield continuous, closed-form controllers. The minimum safe distance is a smooth analytical function that does not require optimization or discrete algorithms and whose derivatives can be computed offline. The use of a continuous differentiable shortest distance eliminates the discontinuity of defining critical points or the conservatism of assuming spherical or ellipsoidal shapes. We also provide explicit distance formulas and a simulation example of a pair of planar manipulators.

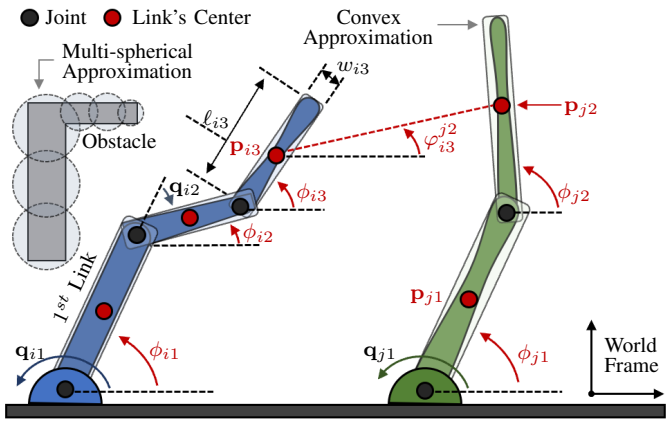

Fig. 1: Planar manipulators with an obstacle. Two shape approximations conventionally used in collision avoidance are represented: the use of a single convex shape on the manipulators and the use of multiple spheres on the obstacle.

II. Preliminaries

We consider the task of coordinating the motion of N n_i-degree-of-freedom (DOF) rigid, nonlinear manipulators with generalized coordinates (or joint configurations) given by

$$\mathbf{q}_i(t) = [q_{i1}(t), \cdots, q_{in_i}(t)]^T, \qquad \text{for } i \in \mathbb{N} \qquad (1)$$

where $\mathbb{N} = \{1, \cdots, N\}$ denotes the set of robots. The joints and links are labeled in ascending order from the most proximal to the most distal, as seen in Fig. 1. The position of the geometric center of each link with respect to a common world reference frame is denoted in Cartesian coordinates by $\mathbf{p}_{ij}(t) := \mathbf{p}_{ij}(\mathbf{q}_i(t)) \in \mathbb{R}^n$, where n is the dimension of the robots' workspace. The joint velocity $\dot{\mathbf{q}}_i(t)$ and the velocity of the geometric center $\dot{\mathbf{p}}_{i_j}(t)$ are related by the translational Jacobian $J_{ij}(\mathbf{q}_i(t)) = \partial \mathbf{p}_{i_j}(t)/\partial \mathbf{q}_i(t)$, i.e., $\dot{\mathbf{p}}_{ij}(t) = J_{ij}(\mathbf{q}_i(t))\dot{\mathbf{q}}_i(t)$.

In addition, we define the angular orientation of each link with respect to the common world frame as

$$\boldsymbol{\theta}_{ij}(t) := [\phi_{ij}(\mathbf{q}_i(t)), \vartheta_{ij}(\mathbf{q}_i(t)), \psi_{ij}(\mathbf{q}_i(t))]^T \quad (2)$$

where ϕ_{ij}, ϑ_{ij}, and ψ_{ij} denotes the orientation of ith robot's jth link in Euler angles with respect to the xy, zx, and yz planes (or, equivalently, about the z, y, and x axes), respectively. Similar to the linear velocities, the angular velocities are related to joint velocities by the rotational Jacobian $\mathcal{J}_{ij}(\mathbf{q}_i(t)) = \partial\boldsymbol{\theta}_{ij}(t)/\partial\mathbf{q}_i(t)$, i.e., $\dot{\boldsymbol{\theta}}_{ij}(t) = \mathcal{J}_{ij}(\mathbf{q}_i(t))\dot{\mathbf{q}}_i(t)$. In what follows, we will omit the time argument of signals.

A. Robot Dynamics

The manipulators are assumed to be fully actuated with nonlinear Lagrangian dynamics given by

$$M_i(\mathbf{q}_i)\ddot{\mathbf{q}}_i + C_i(\mathbf{q}_i, \dot{\mathbf{q}}_i)\dot{\mathbf{q}}_i + \mathbf{g}_i(\mathbf{q}_i) = \boldsymbol{\tau}_i, \qquad i \in \mathbb{N} \quad (3)$$

where $M_i(\mathbf{q}_i) \in \mathbb{R}^{n_i \times n_i}$ are the positive definite inertia matrices, $C_i(\mathbf{q}_i, \dot{\mathbf{q}}_i) \in \mathbb{R}^{n_i \times n_i}$ are the matrices of Coriolis and centrifugal terms, $\mathbf{g}_i(\mathbf{q}_i) \in \mathbb{R}^{n_i}$ are the gravitational torques and forces, and $\boldsymbol{\tau}_i \in \mathbb{R}^{n_i}$ are the control inputs for the ith robot. We assume that $\mathbf{g}_i(\mathbf{q}_i) \in \mathbb{R}^{n_i}$ are known and, therefore, can be compensated via active control and that the manipulators satisfy the following standard properties [2]:

P1. $\exists \bar{m}_i \geq \underline{m}_i > 0$ such that $\underline{m}_i \leq \|M(\mathbf{q}_i)\| \leq \bar{m}_i$,
P2. $\dot{M}_i(\mathbf{q}_i) - 2C_i(\mathbf{q}_i, \dot{\mathbf{q}}_i)$ is skew-symmetric.

B. Control Objective

The main control task for the manipulators is to reach a desired, constant joint configuration, $\mathbf{q}_i^d \in \mathbb{R}^{n_i}$ while avoiding collisions. To this end, we assume that the links can be approximated (or enclosed) by elongated convex shapes, as seen in Fig 1. Furthermore, we assume that adjacent links (i.e., those that share a joint) are offset from each other, which implies that they can move freely without colliding. Using the geometric centers as reference points, we define a minimum safe distance between two non-adjacent links, $\mathbf{p}_{ij}$ and $\mathbf{p}_{kl}$, as

$$r_{ij}^{kl} := r_{ij}^{kl}(\mathbf{p}_{ij}, \mathbf{p}_{kl}, \boldsymbol{\theta}_{ij}, \boldsymbol{\theta}_{kl}) = r_{kl}^{ij}, \quad \text{for } k \in \mathbb{N}, l \in \mathbb{L}_{ij}^k \quad (4)$$

where r_{ij}^{kl} is continuous, differentiable and a function the links' length, depth, and width, and where

$$\mathbb{L}_{ij}^k := \{l \in \{1, \cdots, n_k\} \mid k \in \mathbb{N}/i\} \cup \{l \in \{1, \cdots, n_i\}/\{j-1, j, j+1\} \mid k = i\} \quad (5)$$

represents the set of all non-adjacent links to the ith robot's jth link. It is assumed that this r_{ij}^{kl} is known or can be approximated below. Then, the control objective is to design $\boldsymbol{\tau}_i$ such that $\mathbf{q}_i \to \mathbf{q}_i^d$ as $t \to \infty$ and $\|\mathbf{p}_{ij} - \mathbf{p}_{kl}\| > r_{ij}^{kl}$ $\forall\, t \geq 0$, $j \in \{1, \cdots, n_i\}, k \in \mathbb{N}, l \in \mathbb{L}_{ij}^k$.

III. Collision Avoidance Control

To achieve the control objective, we propose a proportional-derivative (PD) control law with collision avoidance given by

$$\boldsymbol{\tau}_i = \mathbf{g}_i - A_i(\mathbf{q}_i - \mathbf{q}_i^d) - B_i\dot{\mathbf{q}}_i - \sum_{j=1}^{n_i}\sum_{k=1}^{N}\sum_{l \in \mathbb{L}_{ij}^k} \mathbf{u}_{ij}^{kl} \quad (6a)$$

$$\mathbf{u}_{ij}^{kl} = J_{ij}^T\left(\frac{\partial V_{ij}^{kl}}{\partial \mathbf{p}_{ij}} + \frac{\partial V_{ij}^{kl}}{\partial r_{ij}^{kl}}\frac{\partial r_{ij}^{kl}}{\partial \mathbf{p}_{ij}}\right)^T + \mathcal{J}_{ij}^T\left(\frac{\partial V_{ij}^{kl}}{\partial r_{ij}^{kl}}\frac{\partial r_{ij}^{kl}}{\partial \boldsymbol{\theta}_{ij}}\right)^T \quad (6b)$$

where A_i and B_i are positive-definite, diagonal matrices, and $V_{ij}^{kl} := V_{ij}^{kl}(\mathbf{p}_{ij}, \mathbf{p}_{kl}, r_{ij}^{kl})$, known as an avoidance function [4], is given by

$$V_{ij}^{kl} := \left(\min\left\{0, \frac{\|\mathbf{p}_{ij} - \mathbf{p}_{kl}\|^2 - \left(r_{ij}^{kl} + \rho_{ij}^{kl}\right)^2}{\|\mathbf{p}_{ij} - \mathbf{p}_{kl}\|^2 - \left(r_{ij}^{kl}\right)^2}\right\}\right)^2 \quad (7)$$

where $\rho_{ij}^{kl} = \rho_{kl}^{ij} > 0$ is a constant parameter. The radius $r_{ij} + \rho_{ij}^{kl}$ defines the distance at which the ith robot's jth link should start avoiding the kth robot's lth link. The proposed control law (6) guarantees collision avoidance among non-adjacent links at all times.

Proposition 1: Consider a group of N n_i-DOF manipulators with dynamics and control inputs given by (3) and (6). Assume that $\|\mathbf{p}_{ij}(0) - \mathbf{p}_{kl}(0)\| > r_{ij}^{kl}$ for all $i, k \in \mathbb{N}$, $j \in \{1, \cdots, n_i\}$, $l \in \mathbb{L}_{ij}^k$. Then, $\|\mathbf{p}_{ij}(t) - \mathbf{p}_{kl}(t)\| > r_{ij}^{kl}$ $\forall\, t \geq 0$.

IV. Example: n_i-DOF Planar Manipulators

We present an example and provide complete formulas for the case of n_i-DOF manipulators with cylindrical-shaped links. For simplicity and lack of space, we limit the discussion to the case of planar robots.

A. Minimum Safe Distance Function

Consider the interaction of the ijth link with the klth link or obstacle. Let the shape of the ijth link be approximated by a rectangle of length ℓ_{ij} and width w_{ij}, as shown in Fig. 2. Similarly, let the klth link or obstacle be approximated by a rectangle of length ℓ_{kl} and width w_{kl}. Without loss of generality, assume the motion of the links is restricted to the xy-plane and let their lengths be aligned with the x-axis (i.e., when $\phi_{ij} = 0$). Define the following functions

$$\beta_{ij}^{kl} = \frac{\ell_{ij}}{2} + \frac{\ell_{kl}}{2}\sqrt{\varepsilon^2 + \cos^2\tilde{\phi}_{ij}^{kl}} + \frac{w_{kl}}{2}\sqrt{\varepsilon^2 + \sin^2\tilde{\phi}_{ij}^{kl}} \quad (8a)$$

$$\gamma_{ij}^{kl} = \frac{w_{ij}}{2} + \frac{\ell_{kl}}{2}\sqrt{\varepsilon^2 + \sin^2\tilde{\phi}_{ij}^{kl}} + \frac{w_{kl}}{2}\sqrt{\varepsilon^2 + \cos^2\tilde{\phi}_{ij}^{kl}} \quad (8b)$$

where $\varepsilon > 0$ is a small constant such that the derivatives of (8) are well-defined and $\tilde{\phi}_{ij}^{kl} = \phi_{ij} - \phi_{kl}$ is the relative orientation. Let $\varphi_{ij}^{kl} = \operatorname{atan2}(y_{kl} - y_{ij}, x_{kl} - x_{ij})$ be the angle between $\mathbf{p}_{ij} = [x_{ij}, y_{ij}]^T$ and $\mathbf{p}_{kl} = [x_{kl}, y_{kl}]^T$. Then, the equation for a rectangle with sides β_{ij}^{kl} and γ_{ij}^{kl} in polar coordinates ϱ_{ij}^{kl} and φ_{ij}^{kl}, rotated by ϕ_{ij} can be approximated by

$$\zeta_{ij}^{kl} = \sqrt{\varepsilon^2 + (\gamma_{ij}^{kl}\cos(\varphi_{ij}^{kl} - \phi_{ij}) + \beta_{ij}^{kl}\sin(\varphi_{ij}^{ij} - \phi_{ij}))^2} \quad (9a)$$

$$\eta_{ij}^{kl} = \sqrt{\varepsilon^2 + (\gamma_{ij}^{kl}\cos(\varphi_{ij}^{kl} - \phi_{ij}) - \beta_{ij}^{kl}\sin(\varphi_{ij}^{kl} - \phi_{ij}))^2} \quad (9b)$$

$$\varrho_{ij}^{kl} = \frac{2\beta_{ij}^{ij}\gamma_{ij}^{kl}}{\zeta_{ij}^{kl} + \eta_{ij}^{kl} - 2\varepsilon}. \quad (9c)$$

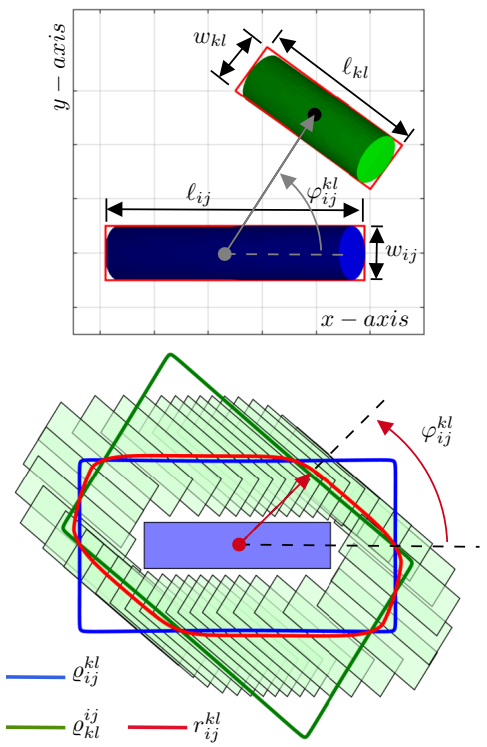

Fig. 2: Minimum safe distance between two cylindrical links.

TABLE I: Parameters for the Planar Manipulators

Parameter	**Robot 1: Links**				**Robot 2: Links**			
	1	2	3	4	1	2	3	4
ℓ_{ij} (m)	1.0	0.5	1.0	0.5	1.0	1.0	0.5	0.5
w_{ij} (m)	0.15	0.15	0.1	0.1	0.15	0.15	0.1	0.1
m_{ij} (kg)	2.0	1.0	2.0	1.0	2.0	2.0	1.0	1.0
Parameters for Traditional Avoidance Control with Spherical Approx.								
# of Spheres	4	3	4	3	4	4	3	3
radius (m)	0.146	0.112	0.135	0.097	0.146	0.146	0.097	0.097

Following the same procedure but using the klth link as the reference, one can obtain a smooth approximation of r_{ij}^{kl}

$$r_{ij}^{kl} = r_{kl}^{ij} = \sqrt[\delta]{\frac{2}{(\varrho_{ij}^{kl})^{-\delta} + (\varrho_{kl}^{ij})^{-\delta}}}, \qquad \delta \geq 2 \tag{10}$$

that is continuously differentiable and bounded. Choosing smaller $\varepsilon \to 0$ and larger $\delta \to \infty$ yields more compact envelopes. The lower half of Fig. 2 illustrates r_{ij} for for the two links when $\tilde{\phi}_{ij}^{kl} = -0.2\pi$. The red line represents the minimum safe distance that the center of the klth link can come from the ijth link, when $\tilde{\phi}_{ij}^{kl} = -0.2\pi$.

B. Simulation

We now simulate the interaction of two distinct 4-DOF revolute planar manipulators with parameters listed in Table I, where m_{ij} denotes the mass of the ith robot's jth link. The manipulators implement the control law in (6), taking into account the safe interactions with a rigid wall at $y = 0\,(\mathrm{m})$ and the centers of each non-adjacent link. The control parameters are then given by $A_i = \mathrm{diag}(9, 6, 4, 4)$, $B_i = \mathrm{diag}(8, 8, 8, 8)$, $\rho_{ij}^{kl} = 0.25\,(\mathrm{m})$, $\varepsilon = 0.02$, and $\delta = 8$, with desired configurations $\mathbf{q}_1^d = [\frac{1}{2}\pi, -\frac{1}{2}\pi, -\frac{1}{2}\pi, \frac{1}{2}\pi]^T\,(\mathrm{rad})$ and $\mathbf{q}_2^d = [\frac{1}{2}\pi, \frac{1}{2}\pi, \frac{1}{6}\pi, \frac{1}{2}\pi]^T\,(\mathrm{rad})$.

The manipulators are first simulated with the proposed control strategy, with results illustrated in Fig. 3(a)-(e). The static wall is simulated as another rectangular link, centered at $x = y = 0\,(\mathrm{m})$, with zero orientation, and with length and width equal to $6\,(\mathrm{m})$ and $0.05\,(\mathrm{m})$. Note that the robotic manipulators are able to successfully converge to the desired configurations while avoiding collisions with each other, with themselves, and with the wall.

For comparison purposes, Fig. 3(f)-(j) show the sequential motion of the manipulators when the traditional artificial potential functions (7) are applied, and the links are approximated by a collection of spheres centered along the links' axes. The number of spheres per link, as well as their radius, are given in Table I, where the location and radius were chosen such that the links are entirely covered. The manipulators avoid all collisions, but as seen in Fig. 3(i) and (j), the manipulators took a longer time to converge to their desired configurations.

Finally, Fig. 4 depicts the norm of the generalized coordinates error and the control torques. Note that, in general, the proposed avoidance control had a slightly faster convergence and lower torques than the case in which links are approximated by multiple spheres and traditional APF functions are applied. This might be due, in part, to the consideration of more APF functions when computing the control torques.

V. Conclusions and Future Work

This paper presented a cooperative, distributed APF-based avoidance control law for multiple robotic manipulators that guarantees collision avoidance at all times. In contrast to previous work, the proposed avoidance control law reduces the conservatism of APF methods by avoiding the traditional spherical and elliptical shape assumptions. Similarly, the control input torques are smooth, well-defined closed-form functions, which simplifies the implementation and avoids discontinuities of other shortest distance-based methods. A simulation example with 2D revolute manipulators demonstrated the performance of the avoidance control strategy in comparison to traditional spherical approximations. In the future, we would like to experimentally validate the proposed avoidance control framework with a physical robot.

References

[1] H. Christensen, et al. A roadmap for US robotics–From internet to robotics 2020 edition. *Foundations and Trends® in Robotics*, 8(4):307–424, 2021.

[2] P. J. From, et al. On the boundedness and skew-symmetric properties of the inertia and Coriolis matrices for vehicle-manipulator systems. In *Proc. IFAC Symp. Intell. Autonomous Vehicles*, Leece, Italy, September 2010.

[3] O. Khatib. Real-time obstacle avoidance for manipulators and mobile robots. *Int. J. Robot. Res.*, 5(1):90–98, 1986.

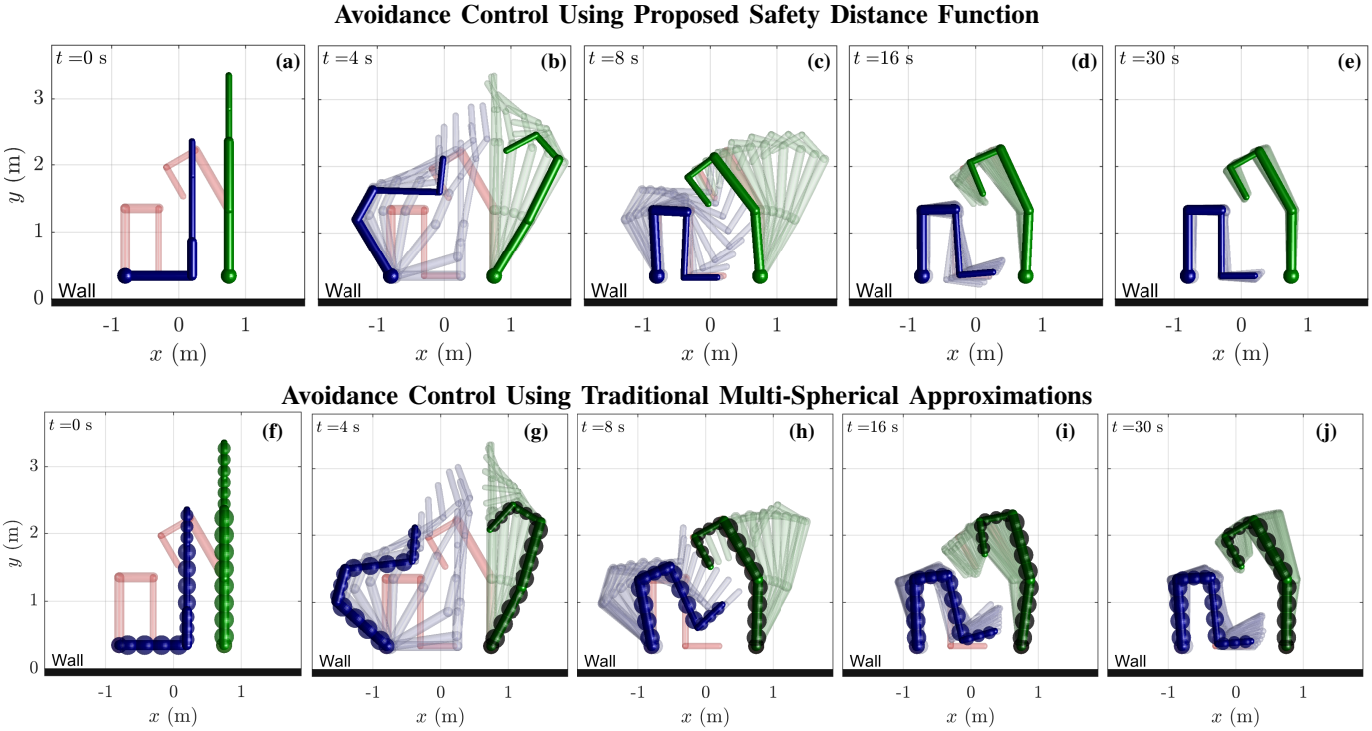

Fig. 3: Simulation of two 4-DOF planar robots interacting with a wall. The top row (a)-(e) illustrates the case of the proposed avoidance control, while the lower row (f)-(j) depicts the use of APF functions (7) with links approximated by a collection of spheres. The first and second robots are denoted in blue and green, respectively, with desired configurations in red. The sequential motion of the manipulators is depicted by the transparent configurations time-spaced by $0.5\,(\mathrm{s})$.

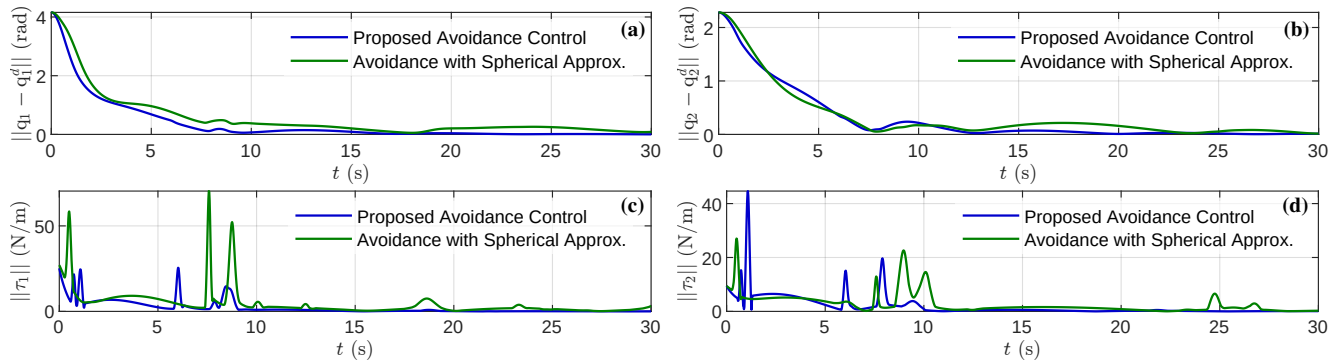

Fig. 4: Vector Norm of the Configuration Errors and Control Torques for the Two Planar Manipulators.

[4] D. M. Stipanović, et al. Cooperative avoidance control for multiagent systems. *J. Dyn. Syst. Meas. Control*, 129: 699–707, September 2007.

[5] W. Wang, et al. An improved artificial potential field method of trajectory planning and obstacle avoidance for redundant manipulators. *Int. J. Adv. Robot. Syst.*, 15(5): 1–13, 2018.

[6] H. Xie, et al. Real-time collision avoidance for a redundant manipulator in an unstructured environment. In *IEEE/RSJ IROS*, pages 1925–1930, 1998.

[7] W. Zhang, et al. Avoidance control with relative velocity information for lagrangian dynamics. *J. Intell. Robot. Syst.*, 99:229–244, 2020.

[8] T. Zhu, et al. Real-time dynamic obstacle avoidance for robot manipulators based on cascaded nonlinear mpc with artificial potential field. *IEEE Trans. Ind. Electron.*, 2024. in press.

[9] S. Zimmermann, et al. Differentiable collision avoidance using collision primitives. In *IEEE/RSJ IROS*, pages 8086–8093, 2022.